Journal of Physical Chemistry and Functional Materials

Home Page of Journal: https://dergipark.org.tr/jphcfum

Review of Optoelectronic Properties of ZnO Photodetector

*Kishwar Mohammed Wasman[1], *, Bestoon Anwer Hamad Ameen*

Department of Physics, College of Science, University of Raparin, Sulaymaniyah, Iraq

Physics Department, College of Education/ Shaqlawa, Salahaddin University-Erbil, Iraq

**Corresponding author: K. M. Wasman (E-mail kishwar.mhamad@uor.edu.krd)*

ABSTRACT

Photodetection has been gained a lot of attention in the last years biased on a military-wide range and civil application. With essential properties of ZnO which has the wide bandgap, strong radiation hardness, low cost, and good chemical stabilities. ZnO is considered the most successful candidate for UV photodetector. The study of our report is to review photodetectors based on doped ZnO nanostructures and the new advances in ZnO nanostructured generation technique including modification and doping methods with modifications of ZnO photodetector. The final part of this review is about literature reviews were reported in recent years about the optoelectrical property of ZnO nanostructures, because Zinc oxide is an important semiconductor material for optoelectronic and industrial applications, such as solar cells, photosensors, and photodetectors, because of has wide attention due to large and direct bandgap (3.34 eV) at room temperature, high mechanical strength, large binding energy (60 m eV), high thermal conductivity, good transparency, high radiation hardness, and non-toxicity.

ARTICLE INFO

Keywords:
ZnO
Photodetectors
Optoelectrical
Nanomaterial
Photoresponse

Received: 2021-11-22
Accepted: 2022-02-16
ISSN: 2651-3080
DOI: 10.54565/jphcfum.1026868

1. Introduction

Photodetection has drawn wide attention according to its various applications in instruments optical signals, industry, and our daily life. PDs which are devices that generate an electrical signal by converting optical signals have been played a critical role in various applications, such as ozone monitoring, space communications, and water purification [1-4]. Wide bandgap semiconductors such as (ZnS, GaN, and ZnO) have been utilized to fabricate high-performance photodetectors. ZnO as an II-VI semiconductor material has been attracted wide attention because of its direct and large bandgap (3.34 eV) at room temperature, high mechanical strength, large binding energy (60 meV), high thermal, high radiation hardness, good transparency, and non-toxicity [5, 6]. Simple preparation, chemical, and thermal stability of ZnO are favorable properties to generate ZnO PDs [7]. Also, ZnO substances have been, applied to PDs because of their high on/off current ratio, large aspect ratio, recovery rate rapid response, and high photoconductive gain [8]. Detecting substances are required to have perfect sensitivity, good detectability with fast response. The ZnO is doped- by another metal, where it's clearly shown that the conductivities of ZnO nanoparticle has been enhanced on UV light illuminations. Extrinsic impurities added into the ZnO nanostructures have been investigated that intensively enhance the UV photodetector capability. For instance, Shabannia [9] was reported the photoresponse study with a Co-doped ZnO NRs based UV photodetector. RajaLakshmi et al.[10] Who performed a Photoresponse study by doping of ZnO thin film via TMs (Mn, Ni, Co). Dai et al.[11] Studied the nanostructures for photodetector application by synthesized n-type ZnO. In recent years, researchers focus on the fabrication of ZNS because crystal morphology and particle size have important roles in determining its usage. The ZnO physical property can be monitored, controlled with surface modification, and doped by introduced rich surface states, and switchable defects within ZnO resulting in a broader response spectrum in the fields of optics, sensing, and optoelectronics [12]. In general, semiconductor medium ZnO was a highly promising third generation for various applications in optoelectronic and lase behavior at room temperature owing to its large binding energy (60 m eV) [13-15].

ZnO ionization coefficient of the electron-hole collision was lower relative to the semiconductor GaN. ZnO got clear advantages and possible values of application in achieving an improved photodetector signal-to-noise ratio. Photodetectors based on ZnO have attracted significant attention and become one of the research hotspots in the UV detectors field depending on wide bandgap semiconductors.

This study report aims to review photodetectors based on doped ZnO nanostructures with recent advances in ZnO nanostructured generation by various synthesis mechanisms and photoresponse property of photodetectors.

2. Zinc Oxide Nanoparticles

2.1 Approach Preparation of ZnO Nanomaterial's

There are various techniques for obtaining the best quality ZnO nanostructures, many influential forming methods recommended. Due to the growth of the environment, these synthesis techniques divide into the vapor phase and solution-based approaches. ZnO is the most promising candidate for UV application. Photodetector based on ZnO has been drawn wide attention in recent years, based on its wide bandgap (3.37eV), strong radiation hardness, low cost, crystallinity, and crystal phase. The researcher has realized that the sizes of semiconductor compounds as regards the corporation model are inversely proportional to the bandgap energy. This denoted that high control of fabrication conditions to determine the photodetector efficiency [16]. The used method is based on the wanted applications, as various techniques produce various morphology and sizes of ZnO particles. Due to this, physical and chemical parameters such as the precursors, pH, solvent, and temperature have been highly considered. ZnO assortment nanoparticles with different growth-morphology such as nanotubes, nanorods, nanoneedles, nanosphere, nanowires, and nanorings were successfully fabricated [17].

Among the methods to fabricate zinc nanoparticles the easiest and low energy costuming was a solution-based approach. The morphology and nanostructures sizes are simply controlled through revisionism. This simple's approach gives good to control a nanostructures size due to its preparation easily and low cost. This Solution to generating ZnO nanostructures including sol-gel [18], hydrothermal [19], spry pyrolysis [20], precipitation [21] , electrospinning [22], microemulsion [23], flux methods [24], solvothermal [25], microwave[26], wet chemical method[27],electrochemical deposition process[28] and polyol [29]. Among those methods, the sol-gel method, is the high straightforward technique to fabricate ZnO nanostructures due to its high reliability, low costs, simplicity of the process, good repeatability, ease of control of physical Characteristics, low process temperature, good compositional homogeneity, the morphology of nanoparticles and optical properties [30].

The vapor phase is the second approach which includes thermal evaporation [31], physical vapor deposition [32], pulsed laser deposition [33], molecular beam epitaxy [34], chemical vapor deposition [35], chemical vapor deposition enhanced with plasma [36], chemical vapor deposition and metal-organic [37], halide or hydride vapor phase epitaxy [38] and so on. Table 1 shows the effect of various processing processes on the characteristics of zinc oxide.

Table 1. The fabrication methods of zinc oxide.

Methods	Precursors	Particle size nm	Morphology	Ref
Hydro-thermal	Zn nitrate 6. hydrates. Zinc acetate dehydrates. Hydrazine hydrates and ammonia	50-150	Needle-shape and flower-shape	[24]
Precipitation process	Zinc oxide powder, Ammonium bicarbonate NH_4HCO_3	D: 15-25	Hexagonal wurtzite structure, the shape of a flower, and shape of the rod	[39]
Electro-chemicals	Zinc electrode. Oxalic acids dehydrate purified. KCL. NaOH and nitric acid	Cylindrical L; 150–200 Spherical D: 50-100	Cylindrical and spherical shapes	[40]
Sol-gel	Zn $(CH_3COO)_2$. Oxalic acid. Ethanol and methanol	L: ~500, D: ~100	Rod shape	[41]
Chemical Vapor Deposition	Zinc acetate dihydrate, ethanol	D:90 L:564	Shape of Nanorod	[42]
Solvothermal	Zn-acetylacetonate monohydrate. Triethanolamine. Absolute ethanol and octanol	D_{sphere} : ~ 20 L_{rod} ~ 100	Spherical Shape and Rod shape	[43]
Mechanochemical process	Zn chloride, sodium carbonite, Sodium chloride	D: 18-35	Hexagonal structure	[44]
Micro-emulsion	Ethyl benzene acid sodium salt (EBS). Dodecyl benzene sulfonic acid sodium salt. Zn acetate dehydrates. Xylene. Hydrazine and ethanol	D (EBS): 80 & D(DBS):300	Nanorod shape	[23]
Co-precipitation	Tetra-hydrated zinc nitrate.	20–40	Crystal Shape	[45]

Ammonium hydroxide

2.2 Classification of ZnO

Nanoparticle ZnO structures may be categorized as novel substances with rarefied applications in the nanotechnology raff fields [46]. It is possible to separate zinc oxide into zero-dimensional (0D), one-dimensional (1D), two-dimensional(2D), and three-dimensional (3D), Subdivided into ordered structures, planar arrays elongated arrays, and quantum dot arrays, each of these nanomaterial's, respectively. Figure 1 explains the zinc oxides morphology and having different dimensions. Nanofibres, nanorods, nanotubes, nanowires, and nanoneedles comprise one-dimensional ZnO arrays. Zinc oxide can be gained in 2D structures, for instance, nanoplate and nanosheet. Examples of 3D structures of ZnO contain dandelion, coniferous, flower, urchin-like, etc.[47]. Due to their high stability, high electron mobility, and strong mechanical power, with many applications such as Nano-lasers, solar cells, photodetectors, photocatalytic, photovoltaics, and electronic processes [48]. The 3D nanostructures are extremely valuable for chemical sensors for dye-sensitized solar cells and photocatalysis also makes it possible to bear mass in substances based on their large specific surface area [49].

Different ZnO nanostructures including nanorods (NRs) [50], NWs [51], nanotubes (NTs) [52], nanoflakes (NFs) [53] nanobelts (NBs), quantum dots (QDs), nanoparticles (NPs) [54], etc. have been destined for performance supportive of UV PDs. Nanoparticles originally show efficient photoconduction characteristics as compared to balk or thin-film counterparts based on large surface-to-volume ratios. The benefits of 1D and 3D ZnO materials were mixed by this method and led to a higher real surface area. In solar cell application, the dye-sensitized manufacture solar cells, this advanced approach has rendered 3D nanoflower a bright material.

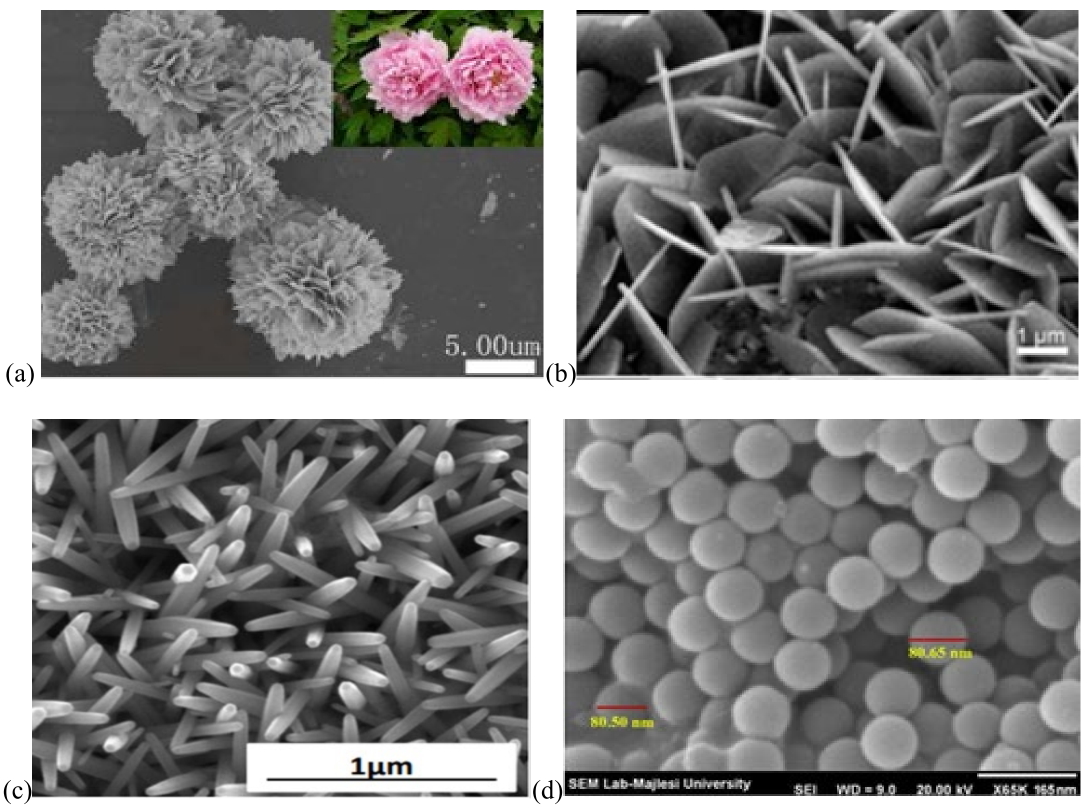

Figure 1. SEM images and FESEM for (a) 3D, (b) 2D[55], (c) 1D[56], (d) 0D[57] zinc oxides.

3. Doping Metal /Nonmetal ZnO Nanostructure

Zinc oxide crystallizes in three forms, cubic zincblende, hexagonal wurtzite, and the rocks salt structures. The wurtzite structure was thermo-dynamically more stable and admirable at ambient conditions [58]. At ambient temperature and pressure, usually, illustrate plan as a planes number of Zn and O ions stack alongside the c-axis while the zinc blende structures are metastable and could be stabilizing through growth on the cubic substrate, but the rock salt structures could be maintained at relatively high pressure [59], these crystal structures are shown in Figure 2, the yellow and blue-shaded spheres symbolize O and Zn atoms, respectively. It has been observed that more electron charge carriers can be given by a larger VO.

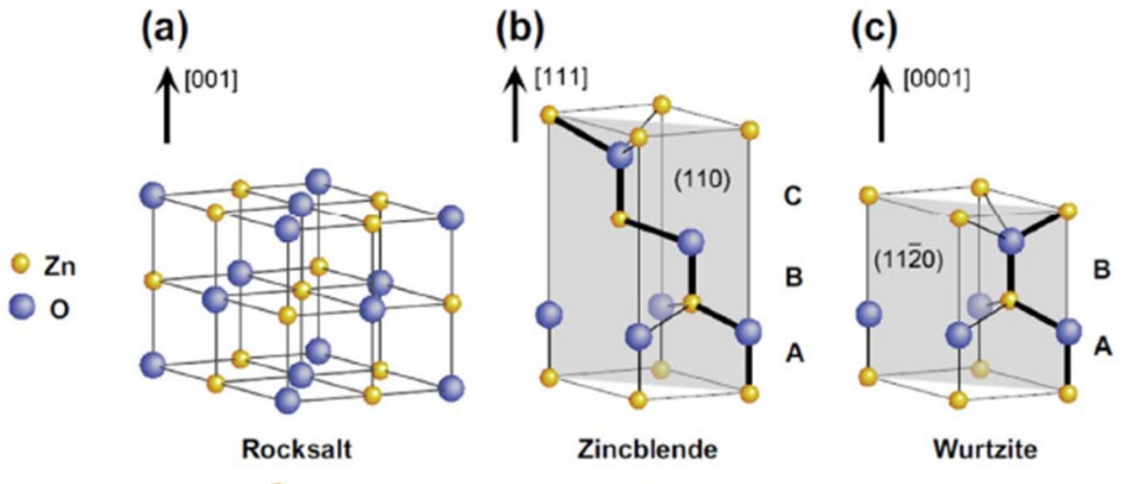

Figure 2. Stick and ball performance of ZnO crystal structures: a) cubic rocksalt (B1), b) cubic zinc blende (B3), c) hexagonal wurtzite (B4) [59].

The intrinsic doping asymmetry of ZnO was studied by Zhang et al. [60]. The intrinsic or extrinsic dopants can be obtained and shown that n-type ZnO through the microscopic equilibrium process. The key obstacles in the manufacture of ZnO semiconductors were difficult for achieving the reliable and reproducible p-type ZnO.

The sol-gel process is used to produce better qualities Ag-N co-doped ZnO. Among the techniques of fabrication, the p-type ZnO synthesize co-doping methods seemed to be critical. Besides this, owing to the different nature of dopants capable of tuning the optical properties of photocatalysts, co-doping has begun to attract extensive interest [61].

One of the most significant factors that increase the sensory reaction of ZnO nanostructures is doping Chang et al. [62]. Metals ions such as Co, Ni, Cu, and Fe were used significantly in ZnO nanostructures as dopants [63]. The dopants not only increase the activity but also modify the resistance of ZnO. Dopants also decrease the sensor's operating temperature, increase its selectivity, stability, and rapid reaction to the target gas [64]. The surface morphology of ZnO nanoparticles is adjusted to the introduction of metal dopants. Owing to the further constraint of crystallite mobility as the borders between the dopant and the host material connect, the particle size of doped Nanoparticles becomes smaller than pristine ZnO nanostructures [65]. Due to the application of dopant, the crystal growth therefore ceases. UV photodetectors characterized by non-ZnO, and silver non-ZnO doped thin film have also been used have or instance defined [66]. In their research, a separate Ag doping content, 0.05, 0.15, 0.65, 1.30, and 2.20 percent by sol-gel technique, has been prepared. They found that the reaction time for low dopant concentration (0.15 percent) decreases dramatically with the introduction of Ag in ZnO and is increased at higher Ag dopant concentration (1.30 percent). That was due to the Ag+ that presumably occupied the Zn2+ sites at quite a low doping concentration within-host ZnO. A detector of photoconductive ultraviolet based on Cu-ZnO doped NR array film via an easy hydrothermal technique and post annealed process was developed by [67]. They observed that Cu-doped ZnO demonstrates an increase in UV detector sensitivity by contrasting the sensitivity of non-doped and Cu-doped NR films. The Cu-doped film of the ZnO NR array indicates 5 repetitive cycles observed by the photocurrent to be stable and repeatable with no degenerative effect during the detection process. In addition, dope ZnO NR array film with Cu will achieve high UV detector efficiency [68] also reported that Photocurrent with dark current values, based on the lithium Li-doping concentrations. They found that the dark current was reduced as the concentration of Li increased. This is attributed to the presence of Zn sites with substitution Li forming holes in ZnO. Recombination between any of these holes and electrons then allowed the LZO thin films to have high resistivity. Their outcome reveals that the photocurrent value improved marginally with an improvement in Li content of up to 2.5 percent and then declined above 2.5 percent. In addition, they find that during on/off switching periods, the photocurrent of pure ZnO thin film is steadily increased. Furthermore, it also claimed that the photocurrent of nondoped ZnO thin film steadily increased and decreased relative to LZO thin film until UV light was turned on and off and did not achieve saturation. According to these results, relative to non-doped ZnO, the LZO thin films demonstrated photocurrent stabilities, rapid photoresponse, and improved reproducibility.

4. Controlling Crystal Growth and Surface Morphology

Various techniques are used to change the size growth and morphology of ZnO to enhance photoactivity. The use of high-quality ZnO crystals will effectively boost PD production by improving the efficiency of light use and reducing the defect.

Several research studies have shown RF sputtering [69], metal-organic chemical vapor deposition (MOCVD)[70], the solution-processed method [54]. Pulsed laser deposition (PLD) [71]. The properties of ZnO-based photodetector can be effectively enhanced based on various fabrication techniques by doping ZnO and annealing crystal to modify their crystal parameter [72]. Photodetector based on Ga-ZnO doped films-based RF sputtered of magnetron demonstrate that the photoresponsiveness of about 2.6 A W-1 in the bias of 10 V in the UV region, with high photoresponse and 10 ns for rising time and 960 ns for decay time with using the pulse illumination. Shinde and Rajpure et al. [73] based spray pyrolysis reported Ga-ZnO thin-film detectors; the high responsivities of it was about 1125 A W-1 at 5 V bias voltages with 365 nm of maximum wavelength. Furthermore, many other materials such as Cu [74], Ti [75], Na [76], Al [77], used for doping ZnO crystals to get detectors of high performance.

Zhou et al. [78] showed that the detector's reset period had been Surface functionalization with the polymers has decreased from 0.8 s to 20 ms. Other types of surface adjustment, such as functionalization of Surface with carbon nanodots [79-82], surface passivation with copper phthalocyanine film [83], HCl treatment [84], and so on, all were stated as feasible methods of obtaining high-performance PDs based on ZnO. Kango et al. also stated that ligand molecules should be shared in this sense. Flower-like ZnO structures, by comparison, have been successfully synthesized Zn2+ molar ratio, and OH− ions are regulated. Flowerlike in a way Then ZnO structures form because of the propensity of nanosheets to minimize their energy on the surface [85].

5. ZnO Coupling with Other Semiconductors

An approach that requires the pairing of two semiconductors is coupled metal oxides of semiconductors such as MxOy/MezOt [86]. Due to higher light absorption, best suppression photoinduced of electrons holes pair recombination, and improved charge separation, nanocomposites were preferable in many applications, especially for photodetector. Shashikant Sharma et al. conducted a study on ZnO/Si heterojunction photodetector efficiency estimation with oxide thickness, temperature, variations in doping profile and studied the effects of parameter variance on photodetector performance [87]. Another related research by Nur et al. [88] also found that it is possible to obtain highly active photocatalysts by combining two semiconductors with separate band gaps.

Hwang et al. [89] Documented an improvement in the photoresponse. It is indicated that the i-ZnO layer effectively decreases the leakage current by around three orders and raises the rectification value from 70 to 6.6 to 104 with p-n and p-i-n photodetectors, respectively, at 2V.49 for both p-i-n and p-n H-photodetector at 0 V and 4 V bias voltages, photocurrent responsivity versus different illumination wavelengths shown in Figure 3(a). The addition of the i-ZnO layer is responsible for the significant increase in UV response for p-i-n HPDs the band-plot of Figure 3(b) and (c) explain the attitudes in p–n and p–i–n in HPDs, respectively, of UV response. A bigger one 2.55 eV valence band offset along with the offset of the conduction band The p-Si/i-ZnO interface of 0.4 eV is considered in these band graphs.

A UV photodetector created from n-ZnO/i-ZnO NR array deposit on the p-GaN layer by using the vapor cooled condensation method has been reported by Chen et al. [4] And further performance improvement is achieved by passivation of photoelectrochemical oxidation. as shown in Figure 3. (d) The peak photoresponsivity is found at 360nm for both unpassivated and passivated ZnO nanorodar ray PDs. For passivated and unpassivated ZnO nanorodar ray photodetectors, the peak photoresponsivity at 360nm is approximately 1.07×102 A/W and 4.37×102, respectively, at zero bias for passivated and unpassivated ZnO NR PDs.

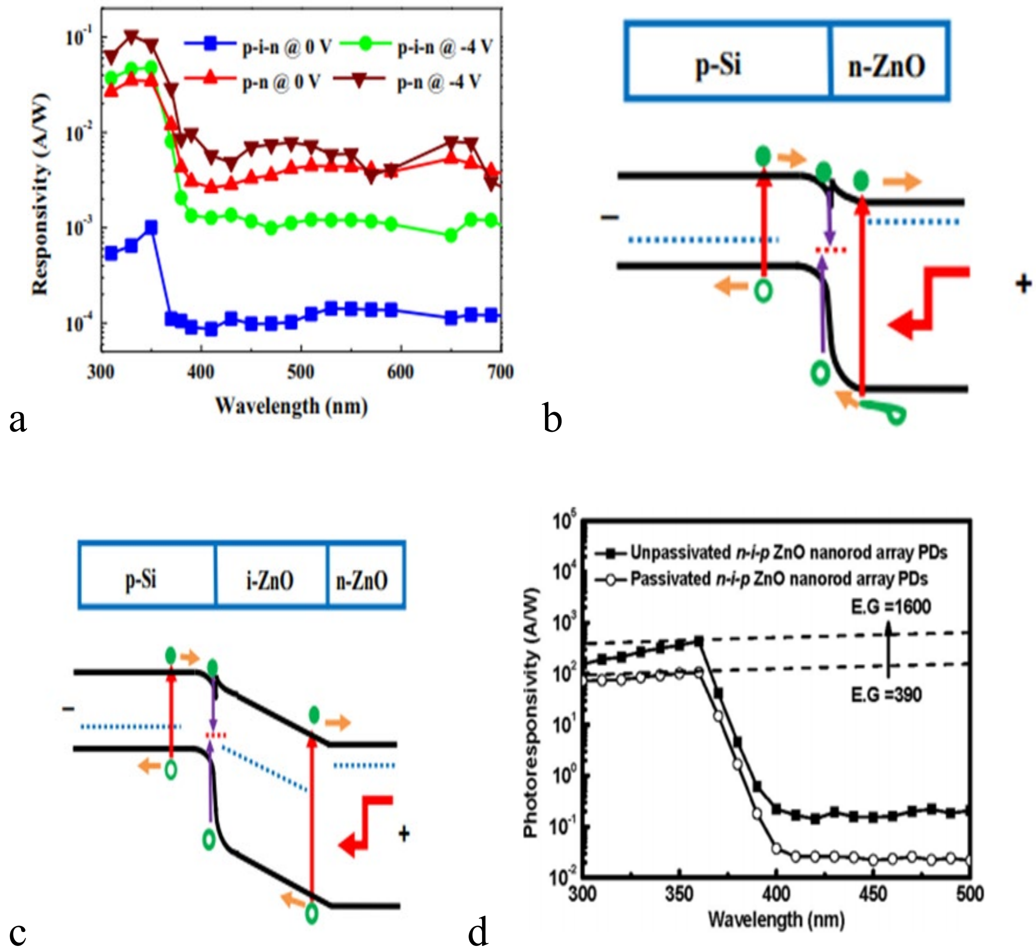

Figure 3 (a)Photocurrent responsively versus different wavelengths of illumination for at 0 V and 4 V bias-voltages, both p-i-n and p-n HPDs, Band-diagrams of HPDs (b) p-n and (c) p-i-n to explain the behaviors of UV-response [89]. d) Passivated and unpassivated n-i-p ZnO NR spectral photoresponsivity Reproduced from Chen, C.-H., Lee, C.-T.,2013 [4].

Array photodetector improving heterostructured ZnO Nanorod/p-GaN efficiency Photodetectors that use an ion passivation process with photoelectrochemical oxide.

6. Optoelectrical Property

Zinc oxide is an important semiconductor material for optoelectronic and industrial applications such as detectors. In recent years the direct bandgap ZnO semiconductors have been extensively studied [90]. wide bandgap materials like ZnO not only gaining most research interest, more than that served as fundamental building in different optoelectronic instruments as well as a photodetector, light-emitting diodes, solar cells, and beam splitting systems nanostructures since of their superior characteristics when generating smaller and further efficient devices [91]. The mechanism of doping into the ZnO has been used to improve the optoelectrical property of ZnO nanoparticles. Bestoon et al. [92] in 2019 reported Solar Light Photodetectors Based Cd-doped ZnO films used sol-gel spin coating method for perpetration they are resulting for each undoped and cd doped ZnO are shown in Figure 4(a) were shows that the transmittance spectra obtained with a solar light wavelength in (200–1200 nm), films showing the transparency about (83%-94 %). 0.1 wt% doping Cd transparency has been maximum, and it improved with low wt % of doping concentration while reducing the transmission by increasing Cd concentration for (4 wt %) that could be concerned within CdO absorption (band-to-band) with such a bandgap lower than ZnO [92].

For direct and indirect transformations, the dependency on the absorption coefficient mostly with photon energies are being studied by optical absorption process, they determined the band gaps of pure and Cd doped samples as shown in Figure 4(b) It was identified that the optical bandgap of the films including Cd material varied from (3.27 to 3.19) eV. While Benyahia, K. Benyahia et al. [93] in 2020 reported Self-powered photodetector by broadband multispectral photoresponsivity based on ZnO-ZnS composite, utilized thermal evaporation technique, UV-Vis-NIR spectroscopy was conducted to determine the optical efficiency of the prepared ZnO-ZnS microstructured composite photodetector, and the related absorbance and reflectance spectra were derived and illustrated in Figure 4(c) and (d), respectively. For fabricated ZnO-ZnS MC the average value of high ability to absorb UV-Vis-NIR was (%72), this result increase exceeds 270% compared to the ZnS film. Also Figure 4(d) shows that in terms of anti-reflection capability, the ZnO-ZnS MC dramatically outperforms the ZnS film, for the ZnO-ZnS increased photons absorption. Whereas lower optical losses have been reported. Light is expanded with better qualities ZnO-ZnS MC deposition the ability to harvest visible and NIR spectrum bands makes it more exciting to produce high photoresponse multispectral photodetector [93]. In the same year, Fatemeh et al. studied high photoresponse UV photodetector based on Ni-ZnO doping Ns, where doped Ni-ZnO Ns prepared by using by thermal decomposition technique, ZnO and Ni-ZnO optoelectronic properties have been assessed in Figure 4(e) shown impact of Ni dopant concentration on the ZnO and Ni-doped ZnO nanoparticle spectrum of UV-Vis In the (300-700) nm range of wavelengths. The Ni-doped ZnO shows a blue shift relative to the pure sample UV-visible spectrum. The optical bang of undoped ZnO and doped Ni was measured using the (E_g=h/mv) formula, the rise in the Ni amount dopant was the source of the expanding band gap of ZnO [94-96]. The bandgap increases from (3.30 - 3.49) eV as dopant concentration has been increased.

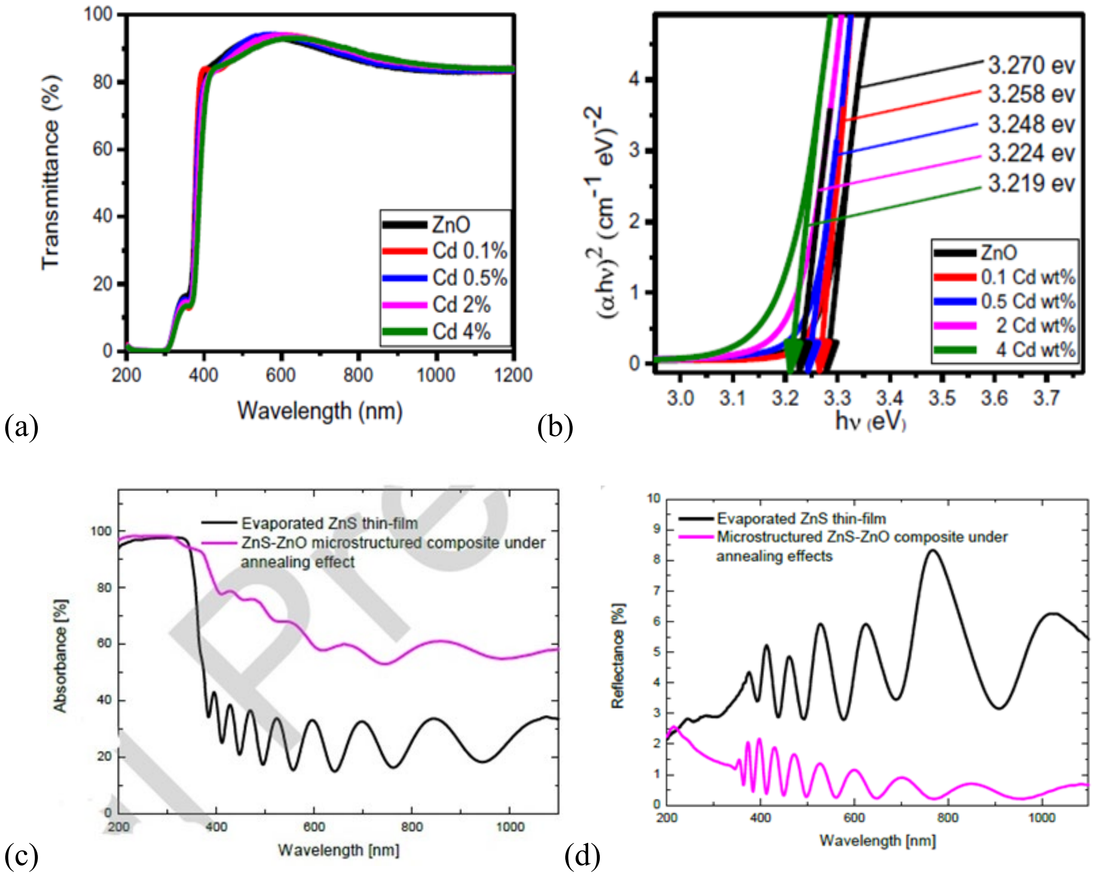

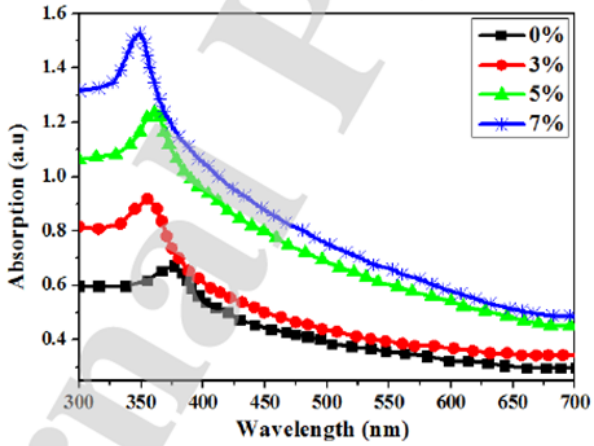

(e)

Figure 4 (a) Transmittances for undoped and cd doped ZnO [92]. (b) Band gape diagram for undoped and cd doped ZnO [92]. (C) Diagram of absorbance and wavelength of ZnO-ZnS MC PD [93]. (d) Graph reflectance and wavelength for undoped zno and ZnO-ZnS [93]. (e) Absorption- wavelength diagram for Ni doped Zno[94].

7. The Photoresponse Properties of ZnO

The identification of the light signal, the bandgap of a photosensitive substance could be smaller or the same as illuminating photon energy. Spectral photoresponse analysis of an ultraviolet photodetector provides its UV signal sensing limits. For photocurrent fabrication, the photogenerated electron and hole require to be separated before recombination with exposure to UV light on the photodetector. The photodetector response current is the current generated by the photodetector under UV illuminations, in which the current is generated just as UV light could be distinguished. Furthermore, the additional photoresponse aperture, responsivity of the photodetector was gives information related to the formation of a response current per unit incident UV lighting power on the photodetector [97]. Bestoon et al. investigated the photoresponse behaviors for undoped ZnO and cd-doped ZnO nanostructures under difference illuminations, I-V behavior of pure and Cd-ZnO Wt% doped shown in Figure 5(a)& (b), respectively. Current enhanced strongly by solar light in reverse bias with solar lighting, this demonstrates that the diode work in a photovoltaic mode, in other words, the diode acts as photocurrent and photovoltage [92]. However, K. Benyahia et al. studied (I-V) characteristics in darkness and under UV-Vis-NIR for ZnO-ZnS MC-based photodetector.

The benefits of improved light scattering with a stronger separation mechanism of the carrier due to the formation heterostructure of ZnO/ZnS have been allowed for ZnO-ZnS MC which is shown in Figure 5c. The illuminated device's I-V curves are converted to 0.15V for negative voltage value, showing its asymmetric photoelectric behavior. The gained photoelectrical characteristic could be ascribed to the potential barrier-induced ZnO-ZnS heterostructure [93]. Fatemeh et al. [94] showed the photocurrent of different voltage characteristics of Ni -ZnO doping nanostructure due to the various Ni concentrations from (−10 V to 10 V) in the dark with UV illumination at (350 nm, 15.5 mW/cm2). The photocurrent change with voltage has been in the shape of the Schottky curve. Low dark currents as 0.15, 0.21, 0.24, and 0.28 nA for various amounts of Ni have been seen at 5V. Biased on the I-V curve, Ni-ZnO doped Ns represent that the conductivity increases with dopant as shown in Figure 5(d). The photocurrent was 53.05, 84.09, 97.36, and 116.52 nA which means an increase in photocurrent gained for Ni doping with decreasing dark current [94].

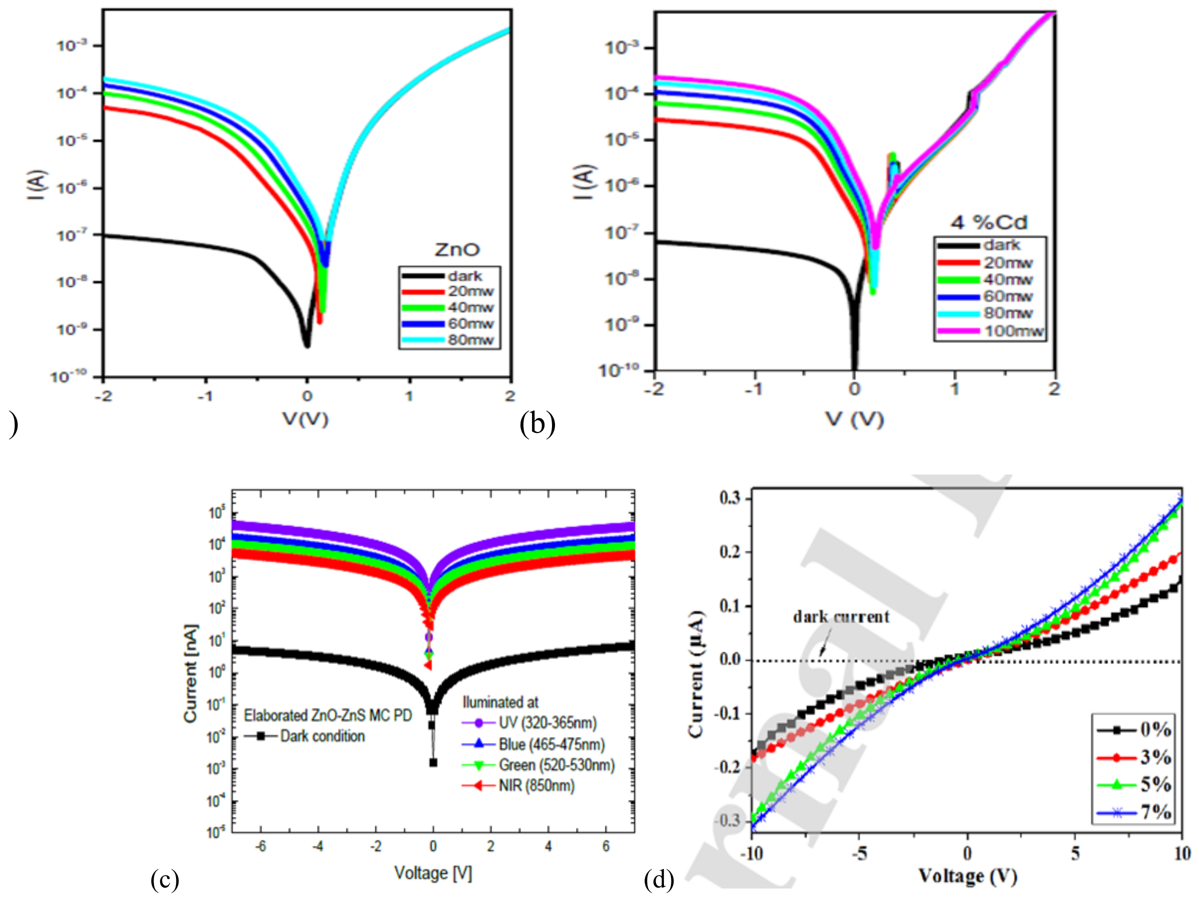

Figure 5. I-V characteristic of undoped and Cd doped ZnO [92], ZnO-ZnS [93] and Ni-doped ZnO [94].

Conclusion

In our review, we summarized the recent publications that research efforts have been focused on the development and efficiency of ZnO-based photodetectors over the past few years. Recently, photodetectors based on ZnO illustrate effective responsivity, low production cost, nontoxic, and capacity for absorbing a solar spectrum greater fraction compared to other semiconductors.

From the generation methods examples were shown in past sections, it was seen that the zinc oxide properties for (3D, 2D, 1D, and 0D) dimension particle size with morphology were affected by the doped fabrication technique.

Among them, fabrication techniques, solution-based doping was beneficial as their capacity to provide the suitable control processes of ZnO growth nanostructures. This was illustrated experimentally by a well-controlled precursor molar ratio.

There are multiple techniques were attempted to improve the nanostructures of ZnO photoresponse. Bandgap energies have been reported to determine a critical factor in ZnO nanoparticle optical property.

It can be concluded that the doping methods are still one of the promising methods to enhance the photodetectors activity doping of nonmetal/metal ZnO. Nevertheless, the study could connect to the theoretical kinetic and experimental to give an improving photodetectors activity of these materials as the application of photodegradation.

These methods enhanced their performance with the shifting of bandgap energies. (Electron-hole) pairs recombination rate, rising efficiency of charge separations, enhanced production rate, generate a smaller particle with better specific surface area.

Acknowledgment

I like to express my special thanks to my family as well as I want to express my thanks to the university of Raparin/college of science /physics department for their helping me in my article review.

Reference

[1] P. Sandvik, K. Mi, F. Shahedipour, R. McClintock, A. Yasan, P. Kung, and M. J. J. o. c. g. Razeghi. AlxGa1− xN for solar-blind UV detectors. 2001;231(3):366-370.

[2] S.-J. Young, L.-W. Ji, S.-J. Chang, and Y.-K. J. J. o. c. g. Su. ZnO metal–semiconductor–metal ultraviolet sensors with various contact electrodes. 2006;293(1):43-47.

[3] C. Varenne, L. Mazet, J. Brunet, K. Wierzbowska, A. Pauly and B. J. T. S. F. Lauron. Improvement in the lifetime of pseudo-Schottky diode sensor: Towards selective detection of O3 in a gaseous mixture (O3, NO2). 2008;516(8):2237-2243.

[4] C.-H. Chen and C.-T. J. I. t. o. n. Lee. Enhancing the performance of ZnO nanorod/p-GaN heterostructured photodetectors using the photoelectrochemical oxidation passivation method. 2013;12(4):578-582.

[5] S.-M. Lam, J.-C. Sin and A. R. J. M. L. Mohamed. Fabrication of ZnO nanorods via a green hydrothermal method and their light driven catalytic activity towards the erasure of phenol compounds. 2016; 167:141-144.

[6] C.-H. Huang, Y.-L. Chu, L.-W. Ji, I.-T. Tang, T.-T. Chu, and B.-J. J. M. T. Chiou. Fabrication and characterization of homostructured photodiodes with Li-doped ZnO nanorods. 2020:1-7.

[7] M. Belhaj, C. Dridi, R. Yatskiv and J. J. O. E. Grym. The improvement of UV photodetection based on polymer/ZnO nanorod heterojunctions. 2020; 77:105545.

[8] W. Kim and K. S. J. P. s. s. Chu. ZnO nanowire field-effect transistor as a UV photodetector; optimization for maximum sensitivity. 2009;206(1):179-182.

[9] R. J. M. L. Shabannia. High-sensitivity UV photodetector based on oblique and vertical Co-doped ZnO nanorods. 2018; 214:254-256.

[10] R. Rajalakshmi, S. J. M. S. Angappane and E. B. Synthesis, characterization and photoresponse study of undoped and transition metal (Co, Ni, Mn) doped ZnO thin films. 2013;178(16):1068-1075.

[11] W. Dai, X. Pan, S. Chen, C. Chen, W. Chen, H. Zhang, and Z. J. R. a. Ye. ZnO homojunction UV photodetector based on solution-grown Sb-doped p-type ZnO nanorods and pure n-type ZnO nanorods. 2015;5(9):6311-6314.

[12] H.-C. Wang, Y. Hong, Z. Chen, C. Lao, Y. Lu, Z. Yang, Y. Zhu, and X. J. N. R. L. Liu. ZnO UV Photodetectors Modified by Ag Nanoparticles Using All-Inkjet-Printing. 2020;15(1):1-8.

[13] S. Yuvaraj, A. C. Fernandez, M. Sundararajan, C. S. Dash, and P. J. C. I. Sakthivel. Hydrothermal synthesis of ZnO–CdS nanocomposites: structural, optical, and electrical behavior. 2020;46(1):391-402.

[14] W. K. Khalef, A. A. Aljubouri, A. D. J. O. Faisal and Q. Electronics. Photo detector fabrication based ZnO nanostructure on silicon substrate. 2020;52(7):1-10.

[15] N. P. Dasgupta, J. Sun, C. Liu, S. Brittman, S. C. Andrews, J. Lim, H. Gao, R. Yan and P. J. A. m. Yang. 25th anniversary article: semiconductor nanowires–synthesis, characterization, and applications. 2014;26(14):2137-2184.

[16] A. J. p. s. s. Verma. An empirical model for bulk modulus and cohesive energy of rocksalt-, zincblende-and chalcopyrite-structured solids. 2009;246(2):345-353.

[17] N. Yahya, H. Daud, N. A. Tajuddin, H. M. Daud, A. Shafie, and P. Puspitasari, editors. Application of ZnO nanoparticles EM wave detector prepared by sol-gel and self-combustion techniques. Journal of Nano Research; 2010: Trans Tech Publ.

[18] Y. Fang, Z. Li, S. Xu, D. Han, D. J. J. o. A. Lu, and Compounds. Optical properties and photocatalytic activities of spherical ZnO and flower-like ZnO structures synthesized by facile hydrothermal method. 2013; 575:359-363.

[19] F. Wang, X. Qin, Z. Guo, Y. Meng, L. Yang and Y. J. C. I. Ming. Hydrothermal synthesis of dumbbell shaped ZnO microstructures. 2013;39(8):8969-8973.

[20] S. Studenikin, N. Golego, and M. J. J. o. A. p. Cocivera. Fabrication of green and orange photoluminescent, undoped ZnO films using spray pyrolysis. 1998;84(4):2287-2294.

[21] Y.-H. Chou, K.-B. Hong, C.-T. Chang, T.-C. Chang, Z.-T. Huang, P.-J. Cheng, J.-H. Yang, M.-H. Lin, T.-R. Lin, and K.-P. J. N. l. Chen. Ultracompact pseudowedge plasmonic lasers and laser arrays. 2018;18(2):747-753.

[22] C. Pan, L. Dong, G. Zhu, S. Niu, R. Yu, Q. Yang, Y. Liu, and Z. L. J. N. P. Wang. High-resolution electroluminescent imaging of pressure distribution using a piezoelectric nanowire LED array. 2013;7(9):752-758.

[23] S. K. Lim, S.-H. Hwang, S. Kim, H. J. S. Par,k and A. B. Chemical. Preparation of ZnO nanorods by microemulsion synthesis and their application as a CO gas sensor. 2011;160(1):94-98.

[24] M. Hasanpoor, M. Aliofkhazraei and H. J. P. M. S. Delavari. Microwave-assisted synthesis of zinc oxide nanoparticles. 2015; 11:320-325.

[25] L. Wan, S. Yan, J. Feng, Z. Yang, X. Fan, Z. Li, Z. J. C. Zou, S. A. Physicochemical and E. Aspects. Solvothermal synthesis of core–shell ZnO hollow microhemispheres. 2012; 396:46-50.

[26] D. Zhang, X. Ni, H. Zheng, Y. Li, X. Zhang, and Z. J. M. L. Yang. Synthesis of needle-like nickel nanoparticles in water-in-oil microemulsion. 2005;59(16):2011-2014.

[27] H. Wu and W. J. J. o. t. A. C. S. Pan. Preparation of zinc oxide nanofibers by electrospinning. 2006;89(2):699-701.

[28] S. Jiao, K. Zhang, S. Bai, H. Li, S. Gao, H. Li, J. Wang, Q. Yu, F. Guo, and L. J. E. A. Zhao. Controlled morphology evolution of ZnO nanostructures in the electrochemical deposition: From the point of view of chloride ions. 2013; 111:64-70.

[29] M. Ushio and Y. J. J. o. m. s. Sumiyoshi. Synthesis of ZnO single crystals by the flux method. 1993;28(1):218-224.

[30] H. Köse, Ş. Karaal, A. O. Aydın and H. J. J. o. P. S. Akbulut. A facile synthesis of zinc oxide/multiwalled carbon nanotube nanocomposite lithium-ion battery anodes by sol–gel method. 2015; 295:235-245.

[31] D. Jiang, J. Zhao, M. Zhao, Q. Liang, S. Gao, J. Qin, Y. Zhao, A. J. J. o. a. Li and compounds. Optical waveguide based on ZnO nanowires prepared by a thermal evaporation process. 2012; 532:31-33.

[32] W. Ouyang and J. J. M. L. Zhu. Catalyst-free synthesis of macro-scale ZnO nanonail arrays on Si substrate by simple physical vapor deposition. 2008;62(17-18):2557-2560.

[33] X. Ma, J. Zhang, J. Lu and Z. J. A. S. S. Ye. Room temperature growth and properties of ZnO films by pulsed laser deposition. 2010;257(4):1310-1313.

[34] W. Changzheng, C. Zhong, H. Haiquan and Z. J. P. B. Dong, Condensed Matter. Effect of the oxygen pressure on the microstructure and optical properties of ZnO films prepared by laser molecular beam epitaxy. 2009;404.

[35] J. J. Wu and S. C. J. A. m. Liu. Low-temperature growth of well-aligned ZnO nanorods by chemical vapor deposition. 2002;14(3):215-218.

[36] P. Hu, N. Han, D. Zhang, J. C. Ho, Y. J. S. Chen, and A. B. Chemical. Highly formaldehyde-sensitive, transition-metal doped ZnO nanorods prepared by plasma-enhanced chemical vapor deposition. 2012; 169:74-80.

[37] C.-H. Lee and D.-W. J. T. s. f. Kim. Thickness dependence of microstructure and properties of ZnO thin films deposited by metal-organic chemical vapor deposition using ultrasonic nebulization. 2013; 546:38-41.

[38] T. Detchprohm, K. Hiramatsu, H. Amano, and I. J. A. p. l. Akasaki. Hydride vapor phase epitaxial growth of a high quality GaN film using a ZnO buffer layer. 1992;61(22):2688-2690.

[39] V. Parihar, M. Raja and R. J. R. o. A. M. S. Paulose. A brief review of structural, electrical, and electrochemical properties of zinc oxide nanoparticles. 2018;53(2):119-130.

[40] V. Anand, V. C. J. J. o. A. Srivastava and Compounds. Zinc oxide nanoparticles synthesis by electrochemical method: optimization of parameters for maximization of productivity and characterization. 2015; 636:288-292.

[41] T. Mahato, G. Prasad, B. Singh, J. Acharya, A. Srivastava, and R. J. J. o. h. m. Vijayaraghavan. Nanocrystalline zinc oxide for the decontamination of sarin. 2009;165(1-3):928-932.

[42] M. Laurenti, N. Garino, S. Porro, M. Fontana, C. J. J. o. A. Gerbaldi and Compounds. Zinc oxide nanostructures by chemical vapour deposition as anodes for Li-ion batteries. 2015; 640:321-326.

[43] S. Gnanam, V. J. J. o. A. Rajendran and Compounds. Facile sol-gel preparation of Cd-doped cerium oxide (CeO2) nanoparticles and their photocatalytic activities. 2018; 735:1854-1862.

[44] A. Stanković, L. Veselinović, S. Škapin, S. Marković and D. J. J. o. m. s. Uskoković. Controlled mechanochemically assisted synthesis of ZnO nanopowders in the presence of oxalic acid. 2011;46(11):3716-3724.

[45] V. Kumar, P. Wariar, V. Prasad and J. J. M. L. Koshy. A novel approach for the synthesis of nanocrystalline zinc oxide powders by room temperature co-precipitation method. 2011;65(13):2059-2061.

[46] Y. Ding, F. Zhang, and Z. L. J. N. R. Wang. Deriving the three-dimensional structure of ZnO nanowires/nanobelts by scanning transmission electron microscope tomography. 2013;6(4):253-262.

[47] A. Kołodziejczak-Radzimska and T. J. M. Jesionowski. Zinc oxide—from synthesis to application: a review. 2014;7(4):2833-2881.

[48] S. M. Ng, D. S. N. Wong, J. H. C. Phung, and H. S. J. T. Chua. Integrated miniature fluorescent probe to leverage the sensing potential of ZnO quantum dots for the detection of copper (II) ions. 2013; 116:514-519.

[49] S. H. Ko, D. Lee, H. W. Kang, K. H. Nam, J. Y. Yeo, S. J. Hong, C. P. Grigoropoulos and H. J. J. N. l. Sung. Nanoforest of hydrothermally grown hierarchical ZnO nanowires for a high efficiency dye-sensitized solar cell. 2011;11(2):666-671.

[50] G. Chai, O. Lupan, L. Chow, H. J. S. Heinrich, and A. A. Physical. Crossed zinc oxide nanorods for ultraviolet radiation detection. 2009;150(2):184-187.

[51] X. Liu, L. Gu, Q. Zhang, J. Wu, Y. Long and Z. J. N. c. Fan. All-printable band-edge modulated ZnO nanowire photodetectors with ultra-high detectivity. 2014;5(1):1-9.

[52] N. Chantarat, Y.-W. Chen, S.-Y. Chen, and C.-C. J. N. Lin. Enhanced UV photoresponse in nitrogen plasma ZnO nanotubes. 2009;20(39):395201.

[53] B. Deka Boruah, A. J. A. a. m. Misra and interfaces. Energy-efficient hydrogenated zinc oxide nanoflakes for

high-performance self-powered ultraviolet photodetector. 2016;8(28):18182-18188.

[54] Y. Jin, J. Wang, B. Sun, J. C. Blakesley and N. C. J. N. l. Greenham. Solution-processed ultraviolet photodetectors based on colloidal ZnO nanoparticles. 2008;8(6):1649-1653.

[55] M. K. Gupta, J.-H. Lee, K. Y. Lee, and S.-W. J. A. n. Kim. Two-dimensional vanadium-doped ZnO nanosheet-based flexible direct current nanogenerator. 2013;7(10):8932-8939.

[56] N. Jalali, J. Briscoe, P. Woolliams, M. Stewart, P. M. Weaver, M. Cain and S. Dunn, editors. Passivation of zinc oxide nanowires for improved piezoelectric energy harvesting devices. Journal of Physics: Conference Series; 2013: IOP Publishing.

[57] S. J. A. J. o. C. Zavar. A novel three component synthesis of 2-amino-4H-chromenes derivatives using nano ZnO catalyst. 2017;10: S67-S70.

[58] A. Moezzi, A. M. McDonagh and M. B. J. C. e. j. Cortie. Zinc oxide particles: Synthesis, properties, and applications. 2012; 185:1-22.

[59] Ü. Özgür, Y. I. Alivov, C. Liu, A. Teke, M. Reshchikov, S. Doğan, V. Avrutin, S.-J. Cho, Morkoç and H. J. J. o. a. physics. A comprehensive review of ZnO materials and devices. 2005;98(4):11.

[60] T.-M. Hong and H.-F. J. P. R. B. Meng. Spin-dependent recombination and electroluminescence quantum yield in conjugated polymers. 2001;63(7):075206.

[61] R. Mereu, A. Mesaros, M. Vasilescu, M. Popa, M. Gabor, L. Ciontea and T. J. C. I. Petrisor. Synthesis and characterization of undoped, Al and/or Ho doped ZnO thin films. 2013;39(5):5535-5543.

[62] C.-J. Chang, C.-Y. Lin, J.-K. Chen, and M.-H. J. C. I. Hsu. Ce-doped ZnO nanorods based low operation temperature NO2 gas sensors. 2014;40(7):10867-10875.

[63] H. Gong, J. Hu, J. Wang, C. Ong, F. J. S. Zhu, and A. B. Chemical. Nano-crystalline Cu-doped ZnO thin film gas sensor for CO. 2006;115(1):247-251.

[64] V. S. Bhati, S. Ranwa, S. Rajamani, K. Kumari, R. Raliya, P. Biswas, M. J. A. a. m. Kumar and interfaces. Improved sensitivity with low limit of detection of a hydrogen gas sensor based on rGO-loaded Ni-doped ZnO nanostructures. 2018;10(13):11116-11124.

[65] A. Maciel, P. N. Lisboa-Filho, E. Leite, C. Paiva-Santos, W. Schreiner, Y. Maniette and E. J. J. o. t. E. C. S. Longo. Microstructural and morphological analysis of pure and Ce-doped tin dioxide nanoparticles. 2003;23(5):707-713.

[66] A. Rajan, H. K. Yadav, V. Gupta, and M. J. J. o. m. s. Tomar. Sol–gel derived Ag-doped ZnO thin film for UV photodetector with enhanced response. 2013;48(22):7994-8002.

[67] W. Dai, X. Pan, C. Chen, S. Chen, W. Chen, H. Zhang, and Z. J. R. A. Ye. Enhanced UV detection performance using a Cu-doped ZnO nanorod array film. 2014;4(60):31969-31972.

[68] W. Lee, J.-Y. J. J. o. N. Leem and Nanotechnology. Ultraviolet Photoresponse Properties of Li-Doped ZnO Thin Films Prepared by Sol–Gel Spin-Coating Method. 2017;17(8):5697-5700.

[69] T. Ghosh and D. J. N. Basak. Highly efficient ultraviolet photodetection in nanocolumnar RF sputtered ZnO films: a comparison between sputtered, sol–gel and aqueous chemically grown nanostructures. 2010;21(37):375202.

[70] S. Liang, H. Sheng, Y. Liu, Z. Huo, Y. Lu and H. J. J. o. c. G. Shen. ZnO Schottky ultraviolet photodetectors. 2001;225(2-4):110-113.

[71] H. Ohta, M. Kamiya, T. Kamiya, M. Hirano and H. J. T. S. F. Hosono. UV-detector based on pn-heterojunction diode composed of transparent oxide semiconductors, p-NiO/n-ZnO. 2003;445(2):317-321.

[72] J. Sun, F.-J. Liu, H.-Q. Huang, J.-W. Zhao, Z.-F. Hu, X.-Q. Zhang, and Y.-S. J. A. s. s. Wang. Fast response ultraviolet photoconductive detectors based on Ga-doped ZnO films grown by radio-frequency magnetron sputtering. 2010;257(3):921-924.

[73] S. Shinde and K. J. A. s. s. Rajpure. High-performance UV detector based on Ga-doped zinc oxide thin films. 2011;257(22):9595-9599.

[74] P. Shewale and Y. J. C. I. Yu. UV photodetection properties of pulsed laser deposited Cu-doped ZnO thin film. 2017;43(5):4175-4182.

[75] P. Shewale, N. Lee, S. Lee, K. Kang, Y. J. J. o. A. Yu and Compounds. Ti doped ZnO thin film-based UV photodetector: Fabrication and characterization. 2015; 624:251-257.

[76] J. Agrawal, T. Dixit, I. Palani, M. R. Rao, and V. J. J. o. P. D. A. P. Singh. Fabrication of high responsivity deep UV photodetector based on Na doped ZnO nanocolumns. 2018;51(18):185106.

[77] M. H. Mamat, Z. Khusaimi, M. M. Zahidi and M. R. J. J. J. o. A. P. Mahmood. Performance of an ultraviolet photoconductive sensor using well-aligned aluminium-doped zinc-oxide nanorod arrays annealed in an air and oxygen environment. 2011;50(6S):06GF05.

[78] J. Zhou, Y. Gu, Y. Hu, W. Mai, P.-H. Yeh, G. Bao, A. K. Sood, D. L. Polla and Z. L. J. A. p. l. Wang. Gigantic enhancement in response and reset time of ZnO UV nanosensor by utilizing Schottky contact and surface functionalization. 2009;94(19):191103.

[79] D. Cammi, K. Zimmermann, R. Gorny, A. Vogt, F. Dissinger, A. Gad, N. Markiewcz, A. Waag, J. D. Prades and

C. J. T. J. o. P. C. C. Ronning. Enhancement of the sub-band-gap photoconductivity in ZnO nanowires through surface functionalization with carbon nanodots. 2018;122(3):1852-1859.

[80] D. M. Mamand and H. M. Qadr. Comprehensive Spectroscopic and Optoelectronic Properties of BBL Organic Semiconductor. Protection of Metals and Physical Chemistry of Surfaces. 2021;57(5):943-953.

[81] H. M. Qadr and D. M. Mamand. Molecular Structure and Density Functional Theory Investigation Corrosion Inhibitors of Some Oxadiazoles. Journal of Bio-and Tribo-Corrosion. 2021;7(4):1-8.

[82] D. MAMAND. Theoretical Calculations and Spectroscopic Analysis of Gaussian Computational Examination-NMR, FTIR, UV-Visible, MEP on 2, 4, 6-Nitrophenol. Journal of Physical Chemistry and Functional Materials. 2019;2(2):77-86.

[83] Q. Chen, H. Ding, Y. Wu, M. Sui, W. Lu, B. Wang, W. Su, Z. Cui and L. J. N. Chen. Passivation of surface states in the ZnO nanowire with thermally evaporated copper phthalocyanine for hybrid photodetectors. 2013;5(10):4162-4165.

[84] S. Chang, R. W. Chuang, S.-J. Chang, C. Lu, Y. Chiou and S. J. T. S. F. Hsieh. Surface HCl treatment in ZnO photoconductive sensors. 2009;517(17):5050-5053.

[85] S. Kuriakose, N. Bhardwaj, J. Singh, B. Satpati and S. J. B. j. o. n. Mohapatra. Structural, optical and photocatalytic properties of flower-like ZnO nanostructures prepared by a facile wet chemical method. 2013;4(1):763-770.

[86] M. R. J. A. i. C. M. f. M. Vaezi and Nanotechnology. Coupled semiconductor metal oxide nanocomposites: types, synthesis conditions and properties. 2011:365-400.

[87] S. Sharma and C. J. J. o. E. D. Periasamy. Simulation study and performance analysis of n-ZnO/p-Si heterojunction photodetector. 2014;19(2014):1633-1636.

[88] H. Nur, I. I. Misnon and L. K. J. I. J. o. P. Wei. Stannic oxide-titanium dioxide coupled semiconductor photocatalyst loaded with polyaniline for enhanced photocatalytic oxidation of 1-octene. 2007;2007.

[89] J. Hwang, D. Wu and S. J. M. S. i. S. P. Hwang. Inserting an i-ZnO layer to increase the performance of p-Si/n-ZnO heterojunction photodetectors. 2015;39:132-135.

[90] N. Tarwal, A. Patil, N. Harale, A. Rajgure, S. Suryavanshi, W. Bae, P. Patil, J. Kim, J. J. J. o. A. Jang and Compounds. Gas sensing performance of the spray deposited Cd-ZnO thin films. 2014;598:282-288.

[91] M. Zhang, D. Zhang and F. J. I. P. T. L. Jing. Hybrid photodetector based on ZnO nanofiber polymers with high spectrum selectivity. 2016;28(15):1677-1679.

[92] B. A. H. Ameen, A. Yildiz, W. Farooq and F. J. S. Yakuphanoglu. Solar light photodetectors based on nanocrystalline zinc oxide cadmium doped/p-Si heterojunctions. 2019;11(1):563-571.

[93] K. Benyahia, F. Djeffal, H. Ferhati, A. Bendjerad, A. Benhaya, A. J. J. o. A. Saidi and Compounds. Self-powered photodetector with improved and broadband multispectral photoresponsivity based on ZnO-ZnS composite. 2021;859:158242.

[94] F. Abbasi, F. Zahedi and M. J. O. C. hasan Yousefi. Fabricating and investigating high photoresponse UV photodetector based on Ni-doped ZnO nanostructures. 2021;482:126565.

[95] D. MAMAND. Determination the bandgap energy of poly benzimidazobenzophenanthroline and comparison between HF and DFT for three different basis sets. Journal of Physical Chemistry and Functional Materials.2(1):32-36.

[96] D. M. Mamand. Investigation of spectroscopic and optoelectronic properties of benzimidazobenzophenanthroline molecule: Fen Bilimleri Enstitüsü; 2020.

[97] B. D. J. N. A. Boruah. Zinc oxide ultraviolet photodetectors: rapid progress from conventional to self-powered photodetectors. 2019;1(6):2059-2085.